Liquid Crystals
Publication details, including instructions for authors and subscription information:
http://www.informaworld.com/smpp/title~content=t713926090

Computer simulation of interactions between liquid crystal molecules and polymer surfaces I. Alignment of nematic and smectic A phases

D. R. Binger; S. Hanna

Online publication date: 06 August 2010

To cite this Article Binger, D. R. and Hanna, S.(1999) 'Computer simulation of interactions between liquid crystal molecules and polymer surfaces I. Alignment of nematic and smectic A phases', Liquid Crystals, 26: 8, 1205 — 1224
To link to this Article: DOI: 10.1080/026782999204237
URL: http://dx.doi.org/10.1080/026782999204237

LIQUID CRYSTALS, 1999, VOL. 26, NO. 8, 1205–1224

Computer simulation of interactions between liquid crystal molecules and polymer surfaces I. Alignment of nematic and smectic A phases

D. R. BINGER and S. HANNA*
H. H. Wills Physics Laboratory, University of Bristol, Tyndall Avenue, Bristol BS8 1TL, UK

(*Received 30 September 1998; in final form 27 February 1999; accepted 15 March 1999*)

Results are presented from computer simulations of liquid crystal molecules in contact with polymeric surfaces. These form part of a study of the complex alignment interactions which operate in liquid crystal displays. The liquid crystal molecules considered are 4-*n*-pentyl-4′-cyanobiphenyl (5CB) and 4-*n*-octyl-4′-cyanobiphenyl (8CB); the polymeric surfaces simulated were crystalline polyethylene, polypropylene, poly(vinyl alcohol) and Nylon 6. Additional simulations were performed using graphite as a substrate. Polyethylene, poly(vinyl alcohol) and Nylon 6 were all found to induce orientation of the 5CB and 8CB molecules parallel to the polymer chain axes, as would be expected from experimental studies. On the other hand, polypropylene induces many different orientations with no clear preference for either. No evidence was found for the alignment of 8CB molecules on graphite substrates, in disagreement both with experimental findings and the results from previous simulations. The nature of the alignment interactions and possible reasons for the observed discrepancies are discussed.

1. Introduction

The operation of a liquid crystal display, and in particular the quality of contrast available, depends on the interaction between the liquid crystal molecules and an alignment layer, which is often made of polymer. The polymer layer is usually treated by rubbing with cloth or fur in the direction that the liquid crystal alignment is required. Two models have been proposed to explain the effect of rubbing on the polymer surface and hence on the alignment. The initial suggestion [1, 2] was that the alignment was caused by microgrooves which were produced by rubbing. Evidence for the microgrooves was provided by electron microscopy. However, since it was quite common to observe alignment when no grooves were found [3], and since striking differences were observed between the aligning behaviour of different polymers, it appeared that an alternative explanation was required.

Castellano [4] suggested that the rubbing process caused partial melting of the top few molecular layers of the polymer, which then became oriented parallel to the applied shear field. Orientation of the liquid crystal was thought to occur through molecular level interactions between the oriented polymer and the liquid crystal. Support for this second model came initially from birefringence studies which were consistent with the idea that the polymer surface had become oriented. However, more recently grazing-incidence X-ray scattering studies [5–7] have given a direct demonstration of the formation of ordered oriented structures in the surface layers of rubbed polyimides.

While it is clear that both of the above models are capable of explaining the occurrence of liquid crystal alignment, it seems likely that the latter model, involving orientation of the polymer surface, is of most relevance in polymeric systems. However, the nature of the interactions involved between liquid crystals and polymers is not well understood, and there is a need for a detailed, molecular level explanation for the occurrence of liquid crystal alignment.

Some attempts to use computer simulation to understand the organization of liquid crystal molecules on crystalline surfaces have already been carried out. Cleaver *et al.* [8, 9] have considered the interaction between the nematogen 4-*n*-octyl-4′-cyanobiphenyl (8CB) and a graphite substrate in some detail using molecular mechanics and dynamics. Through a careful use of energy minimizations, they were able to observe registration between the 8CB molecules and the substrate, in agreement with images from scanning tunnelling microscopy (STM) [10–13]. Yoneya and Iwakabe [14] have performed molecular dynamics studies on the same system and also reported evidence of alignment. In addition they have studied 8CB molecules in contact with close

*Author for correspondence; e-mail: s.hanna@bristol.ac.uk

packed layers of polyimide and polyamide chains on graphite substrates [15, 16]. Their main finding was that the 8CB molecules preferred to align parallel to the polymer chain axis, with carbonyl units in the polymer providing the main adsorption sites.

The aim of this paper will be to perform a more systematic study of the local interactions between liquid crystal molecules and a variety of polymer surfaces, with a view to identifying the general principles which determine the degree of molecular alignment that may be found. To this end, results will be presented from molecular dynamics simulations of 8CB and 5CB molecules interacting with the crystalline surfaces of polyethylene, poly(vinyl alcohol), polypropylene and Nylon 6. In addition, graphite surfaces will be studied in order to provide comparisons with previous experimental and computational work. A future publication will examine alignment interactions in liquid crystal systems which form smectic C phases [17].

2. Methods and models

Molecular dynamics and mechanics simulations were used to study the interactions of rod-like liquid crystal molecules with several polymer substrates and graphite. Two types of simulation were performed: those involving a single molecule on a polymer surface, and those involving a monolayer of molecules. The single molecule simulations provided a guide to the set of preferred configurations of the molecule on the surface, when unconstrained by the presence of other liquid crystal molecules. The larger simulations demonstrated the additional influence of neighbouring molecules on the orientational preferences of the system. Details of the molecules and polymers considered are given below, together with an explanation of the methods of simulation and analysis.

2.1. *Molecules and surfaces considered*

The liquid crystal molecules considered were 4-*n*-pentyl-4′-cyanobiphenyl (5CB) and 4-*n*-octyl-4′-cyanobiphenyl (8CB) (see figure 1). These molecules were chosen for their simplicity as mesogenic molecules and because they have been widely studied experimentally [18–21]. A comparison between simulations of the two molecules allows the effect of the alkyl tail length to be examined, and with this in mind some simulations were also performed using an isolated cyanobiphenyl core (CB). In the bulk, 8CB forms both smectic and nematic mesophases ($Cr \xleftrightarrow{21.5\,^{\circ}C} SmA \xleftrightarrow{33.5\,^{\circ}C} N \xleftrightarrow{40.5\,^{\circ}C} I$) whereas 5CB displays only a nematic mesophase ($Cr \xleftrightarrow{24\,^{\circ}C} N \xleftrightarrow{35.3\,^{\circ}C} I$) [18].

A range of polymer surfaces were examined. The bulk of the work presented here was performed using a polyethylene (PE) substrate, which is capable of inducing a planar liquid crystal alignment. While PE is not used commercially as an alignment layer, the simplicity of its structure makes it an ideal model system for this investigation. Nylon 6 and poly(vinyl alcohol) (PVA) were chosen because they are also known to induce a planar alignment in liquid crystals [3], and are commonly used in liquid crystal cells. On the other hand, polypropylene (PP) was selected as a polymer that is not reported to give a planar alignment and can, in fact, induce a homeotropic alignment in some systems [22]. Graphite was also examined in order to draw comparisons with previous simulations [8, 9, 14–16] and results from scanning tunnelling microscopy [10–13].

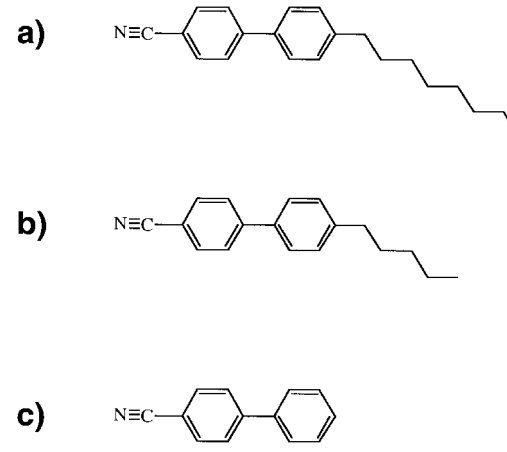

Figure 1. Molecules of (*a*) 8CB (*b*) 5CB and (*c*) CB.

2.2. *Construction of polymer surfaces*

The greatest difficulty in constructing realistic models of polymer surfaces is that there is generally no direct experimental evidence of the surface structures for guidance. As indicated in the introduction, it is now broadly accepted that rubbing a polymer surface can induce orientation of the molecules, at least in a thin surface layer [3–7, 23–25]. Since chain orientation promotes crystallization [26] and semi-crystalline polymers align liquid crystals more effectively than glassy polymers [3, 27] it is not unreasonable to expect the surface morphology to resemble that of one of the crystal faces of the polymer. The question then remains as to which crystal face is most likely to be found. For each of the polymers considered, additional arguments were used to justify the selection.

The crystal structure of PE is shown in figure 2(*a*), projected onto a plane perpendicular to the chain axes. The (1 0 0) and (1 1 0) crystal faces are indicated. These were selected because they are the main crystal growth faces [28]. In addition, studies of the epitaxial growth of molecular crystals on the surface of extruded PE indicate the presence of (1 1 0) faces [29]. Molecules

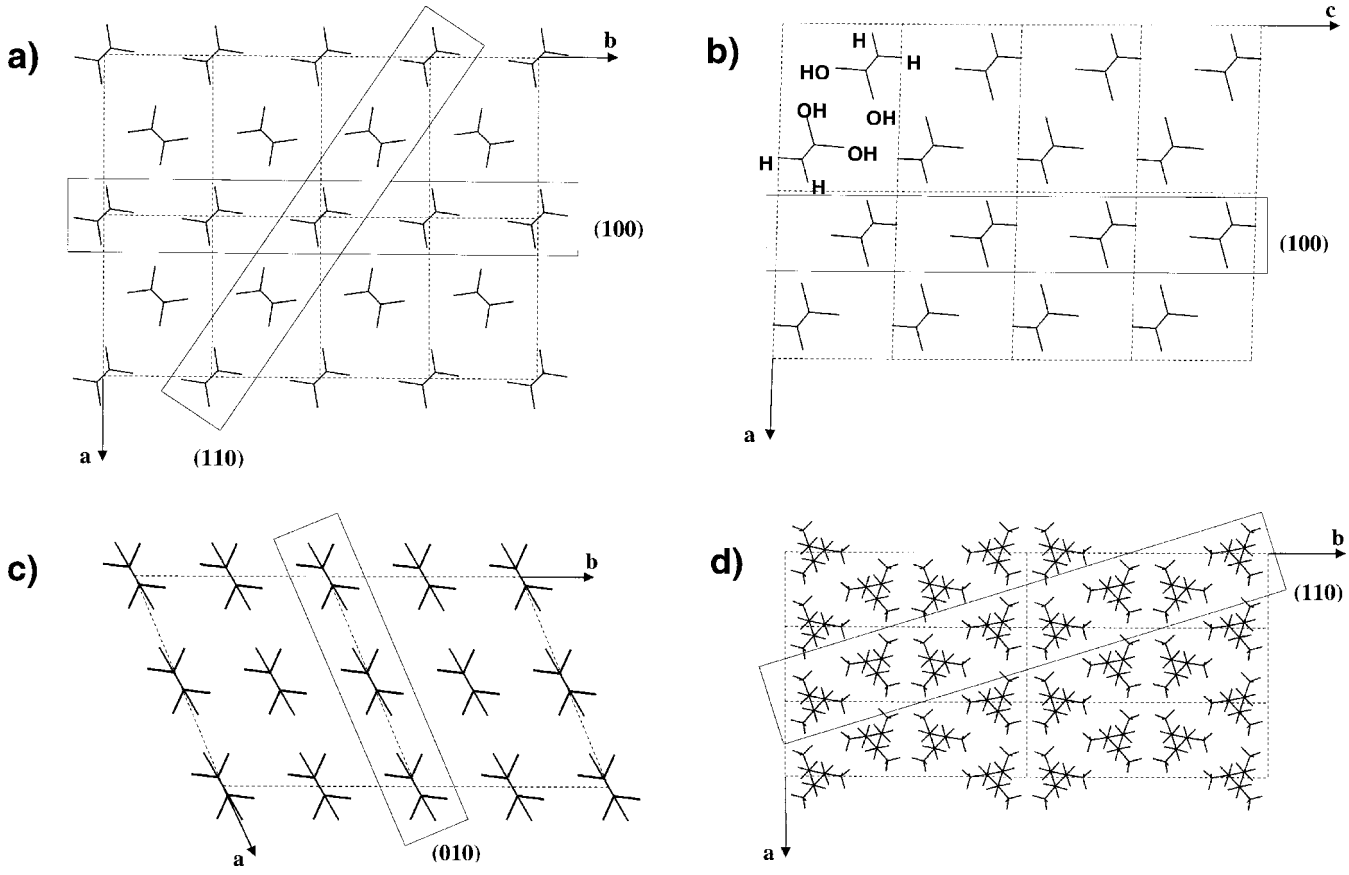

Figure 2. The crystal structures of the polymers used as substrates in the simulations. All polymer chains are viewed end-on, and hydrogen atoms are shown. (*a*) The unit cell of polyethylene projected onto (0 0 1); the (1 0 0) and (1 1 0) planes are indicated. (*b*) The unit cell of PVA projected onto (0 1 0); the positions of the hydroxyl groups are shown, as is the (1 0 0) surface used for the simulations. It should be noted that it is the upper surface which is in contact with the liquid crystal molecules, i.e. the surface which does *not* contain the hydroxyl groups. (*c*) The unit cell of Nylon 6 projected onto (0 0 1); the chains form hydrogen-bonded sheets parallel to the (0 1 0) plane. (*d*) The unit cell of polypropylene projected onto (0 0 1), showing the (1 1 0) plane used for simulation. Molecular images created using Cerius^2.

of PVA have a similar structure to those of PE, with hydroxyl groups replacing hydrogens on every other carbon atom [30]. These hydroxyl groups result in the formation of a double layered sheet structure in the crystal parallel to (1 0 0), see figure 2(*b*). The surface taken for the simulations was therefore the (1 0 0) crystal face, selected so that the non-polar side of the chains, i.e. the upper surface in figure 2(*b*), was in contact with the liquid crystal molecules. A key feature of the structure of Nylon 6, is that it forms hydrogen bonded sheets parallel to the (0 1 0) planes of the crystal, see figure 2(*c*). The (0 1 0) face was thus thought to be a reasonable choice to study here, since there would be a large energy penalty involved in breaking the hydrogen bonds to form other faces. PP was the only polymer for whose surface direct experimental measurements were available. Snétivy *et al.* [31, 32] performed atomic force microscopy (AFM) on isotactic PP samples which were oriented by stretching and then ultra-microtomed. By comparing AFM images with computer models, they were able to identify the dominant cleavage plane as the (1 1 0) plane. Therefore, we have chosen this plane for our simulations, see figure 2(*d*). A summary of all of the surfaces chosen for the simulations is given in table 1.

The coordinates of the atoms in the polymer surfaces were obtained from published crystallographic data [30, 33–35]. Since the exact positions of the hydrogen

Table 1. A summary of the materials and crystal faces used as substrates in the alignment simulations.

Material	Crystal face
PE	(1 1 0), (1 0 0)
Nylon 6	(0 1 0)
PVA	(1 0 0)
PP	(1 1 0)
Graphite	(0 0 1)

atoms were not reported, they were added manually when required, in low energy conformations.

2.3. *Simulation methods*

The molecular dynamics simulation method was used for all of the simulations presented here. Although we considered using Monte Carlo techniques for the single molecule simulations, these would have been less appropriate for the monolayer work, and so the idea was rejected in favour of having a consistent numerical approach for all of the studies. The computer simulations were performed using the Cerius^2 molecular modelling package [36], in conjunction with the Dreiding 2 force field [37]. The functional form of the force field is summarised in table 2. Computing time was saved through the use of a united atom representation of the CH, CH_2 and CH_3 groups. The validity of this approximation was tested by performing some additional simulations with explicit hydrogen atoms. The force field parameters used were those quoted by Mayo *et al.* [37], with the exception of the biphenyl torsional energy term, which will be described below. For the non-bonded terms, a cut-off radius of 8.5 Å was used. To save further computing time, the atoms in the polymer surfaces were not allowed to move during the simulation and only one layer of polymer molecules was considered, significantly reducing the total number of atoms involved in the force calculation. Two-dimensional periodic boundary conditions were applied in the plane of the surface, with the size of the model being large enough to prevent a molecule from interacting with its periodic image.

The Dreiding 2 force field was chosen for the project because of its simplicity, and because it was readily available within the Cerius^2 molecular modelling package. The Dreiding 2 force-field was originally validated using a selection of small molecules which included the biphenylyl and alkyl groups found in 8CB and 5CB [37], and was generally found to provide reliable estimates of both molecular geometries and energy barriers. Since the main aim of the project was to study the gross features of the behaviour of liquid crystal molecules on polymer substrates, the use of more complicated force-fields with large numbers of additional terms, such as the stretch–bend, stretch–torsion, bend–torsion and bend–bend terms that are found in the MM2 and MM3 force-fields [38], was felt to be unjustifiable. In fact, during the course of the project, it became clear that quite fundamental changes to the force-field, i.e. the inclusion or exclusion of electrostatic interactions, or the use of explicit hydrogen atoms rather than united atoms, had little effect on the generic behaviour of the liquid crystal molecules. For this reason, it was decided not to invest time and resources in exploring alternative force fields, but rather, to use a consistent approach across all of our simulations. However, in the future, as it becomes possible to simulate larger and more physically realistic models, the selection of an accurate force-field may be expected to become more important.

Table 2. A summary of the functions used to calculate the potential energy of the system in the Dreiding 2 force field.

Energy term	Functional form
Bond length	$E(r) = \frac{1}{2} c_b (r - r_b)^2$
Bond angle	$E(\theta) = \frac{1}{2} k_\theta (\theta - \theta_0)^2$
Bond torsion	$E(\phi) = \sum_{n=1}^{6} \frac{1}{2} b_n [1 - d_n \cos(n\phi)]$
Van der Waals	$E(r) = d_0 \left[\left(\frac{r_0}{r} \right)^{12} - 2 \left(\frac{r_0}{r} \right)^{6} \right]$
Electrostatic	$E(r) = c_0 \frac{q_i q_j}{\varepsilon r}$

For the systems considered here, the torsional potential in table 2 was simplified and only a single term in the expansion was used:

$$E(\phi) = \frac{1}{2} b [1 - d \cos(n\phi)].$$

For the alkyl chains, we took $n = 3$ with $b = 2$ kcal mol^{-1} and $d = -1$. This choice of torsional potential would appear, at first sight, to give equal weight to the *trans*- and *gauche*-conformations in the alkyl tail. However, the presence of non-bonded interactions along the chain ensures that the *trans*-conformation is preferred at ambient temperatures. In the case of the dihedral angle between the two rings in the biphenyl, the torsional terms were altered to $n = 4$, $b = 25$ kcal mol^{-1} and $d = -1$, thus favouring a non-copolanar configuration. This modification was necessary to compensate for the use of united atoms in the phenyl rings. Without it, the biphenyl group became planar, which was known to be incorrect [39]. A similar problem was reported by Komolkin *et al.* [40] in simulations of bulk 5CB.

Partial atomic charges were calculated for each molecule and substrate, using either the MOPAC semi-empirical molecular orbital package [41] or the Gasteiger electronegativity method [42]. The charges obtained by both methods were found to be comparable. However, since there are no polar sites in the PE and PP surfaces, it was felt that electrostatic interactions could be ignored in these cases.

As indicated above, two types of simulation were performed: those with an isolated molecule on a surface,

and those with monolayers. The procedures followed were different in each case. For the single molecule studies, the liquid crystal molecule freely explored all orientations on the polymer surface. However, the mean rotation times in the plane of the surface were of the order of 1 ns, making it difficult to obtain good statistics. Therefore, in these cases, the results from 16 simulations with uniformly distributed starting orientations were combined, to give total data collection times of 4 ns for each single molecule simulation. Each of the individual simulations was equilibrated for 100 ps prior to data collection, which was sufficient to ensure that all memory of the initial orientation was lost. However, the equilibration of the separate runs was no guarantee that the orientation distribution functions (ODFs) calculated from the molecular dynamics trajectories had converged to their final shapes. In fact, convergence of the ODFs was assessed by noting that ODFs calculated from independent sets of simulations were qualitatively similar, although the exact peak heights showed statistical variations, and that the ODFs obtained for 8CB, 5CB and CB all showed the same features. By proceeding in the above manner, we were able to ensure that the molecule had the opportunity to explore all possible orientations on the polymer surface, while keeping the simulations to a reasonable length.

For simulations with monolayers, it was recognised that the molecules would be unable to explore all possible orientations within the time scale of a simulation, which in the present work was 1 ns. Therefore, we chose to start the monolayer simulations close to the most preferred orientations, as indicated by the ODFs for the single molecules. Thus, the starting configurations for the monolayer simulations were likely to be close to equilibrium. The systems were equilibrated for 100 ps before data were collected. After the initial equilibration period, the ODFs were found not to vary substantially with simulation time, apart from the usual statistical variations. In fact, as will be discussed in more detail below, it was found that the same ODFs were obtained even when the simulations were given very unfavourable starting configurations.

United atom simulations were performed with a simulation time step of 2 fs, while explicit hydrogen atom simulations used a time step of 1 fs. The simulation temperature was set at 300 K except where stated otherwise, corresponding to the smectic A phase of 8CB and the nematic phase of 5CB, and the microcanonical ensemble was used. The simulations were carried out on a variety of desktop Unix workstations, as well as a Silicon Graphics Origin 200 server. The molecular images shown in the figures were generated using the PovChem ray-tracing program [43].

2.4. *Analysis of results*

The most important function determined from the molecular dynamics trajectories was the orientational distribution function (ODF) of the liquid crystal molecules, which was calculated separately for the cores and the tails, and summarizes the orientations explored during each simulation. The orientation of each molecular fragment was found by diagonalizing its moment of inertia tensor. A knowledge of the sequence of the atoms in each fragment enabled its orientation to be determined in the range 0° to 360°. The ODFs are presented here as polar plots, in which the square root of the frequency is plotted versus angle, and the areas of the plots are normalized. By this means, the area of any peak in the ODF will be proportional to the number of configurations contributing to it. However, where peak positions and widths are quoted, these were measured from simple rectangular plots of frequency versus angle, which are not shown.

For the monolayer simulations, the ODF was averaged over all fragments of a particular type in the model. Translational correlation functions were calculated for the liquid crystal molecules in directions both parallel (longitudinal) and perpendicular (lateral) to the polymer chains. Orientational order parameters, $\langle P_2 \rangle$, were calculated from the ODFs for the liquid crystal cores. The ODFs were weighted with $\sin(\alpha)$, where α is the angle between the preferred orientation direction and the liquid crystal long axis, in order to compensate for the fact that the liquid crystal molecules are constrained to two dimensions [44]. The $\langle P_2 \rangle$ values calculated in this manner may be compared directly with values measured in the bulk. In general, it was found that if the order parameters are calculated for the whole molecules, the values obtained are slightly higher than those given below, because the moment of inertia of the whole molecule shows less variation than either of its constituent parts. However, since order parameters are usually obtained from optical measurements, it seems reasonable to quote order parameters derived from the optically anisotropic parts of the molecules.

3. Results

3.1. *Interactions of isolated molecules with PE surfaces*

Typical ODFs for the 8CB molecule on the (1 0 0) and (1 1 0) faces of PE are shown in figure 3, with the positions of the main peaks in the distributions being summarized in table 3. It can be seen that the molecular tails prefer to align parallel to the polymer chain axis in the substrate, i.e. at 0° or 180°. However, the mesogenic cores behave differently, being offset by up to 30° to either side of the chain axis. On the (1 1 0) surface, the mesogenic core lies symmetrically to either side of the

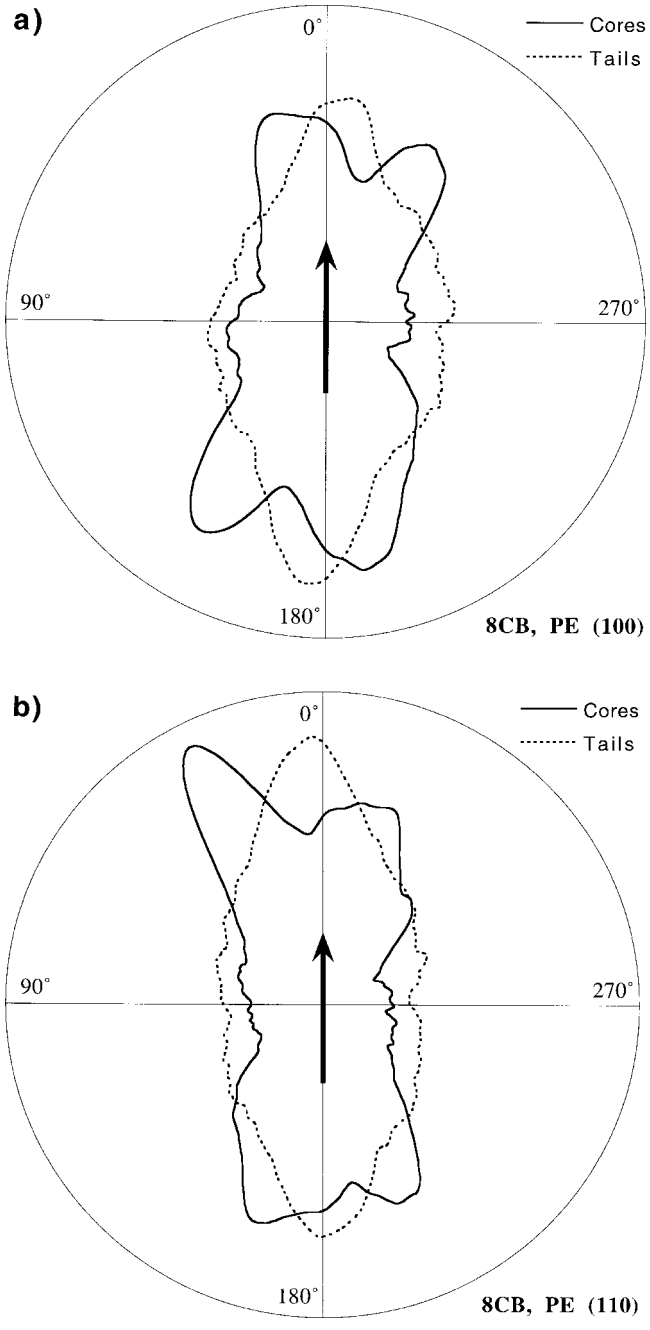

Figure 3. Typical ODFs for a single 8CB molecule on (*a*) the (1 0 0) surface and (*b*) the (1 1 0) surface of PE, using the united atom model. The distributions for the cores are shown as solid lines, while those for the tails are shown as dashed lines. The polymer chain axis is indicated by a vertical arrow through the centre of the plot.

chain axis, whereas, on the (1 0 0) surface, the orientation is asymmetric, with the core taking up positions approximately 5–10° to one side of the chain axis and 20°–30° to the other. The asymmetry found on the (1 0 0) surface disappears when the simulations are performed using explicit hydrogen atoms, whereas the results for the (1 1 0) surface remain symmetrical irrespective of the choice of model (see table 3). Peaks are also observed in the ODF corresponding to a parallel alignment of the cores when using the explicit hydrogen model. The behaviour of the cores described above should be contrasted with that reported in a preliminary study [45], in which a single broad peak was observed centred on the chain axis. The reason for this discrepancy appears to be that the number of independent configurations considered in the preliminary communication was very limited compared with the current work.

The results for the 5CB molecules showed the same general trends as the 8CB molecules, with the tails aligning parallel to the polymer chain direction and the cores offset by up to 30°, see figure 4(*a*). The main difference between the two molecules appears to be that the tail distributions for the 5CB molecules are broader than for the 8CB molecules. This may be an indication that the shorter tails are less well anchored to the substrate. Indeed, the rotational mobility of the 5CB molecules was found to be approximately twice that of the 8CB molecules during the simulations. The behaviour of the isolated CB core was very similar to that of the cores in the liquid crystal molecules, demonstrating a clear preference to align at an angle to the polymer chains, as shown in figure 4(*b*).

The behaviour of the liquid crystal molecules is somewhat unexpected and requires further consideration. The premise behind the construction of the polymer surfaces is that the polymer chain axis will coincide with the direction of rubbing in a real device. Thus it would be expected that the preferred orientation of the mesogenic core would be parallel to the chain axis. In fact this is not the case. Rather, it is the tail that assumes an alignment parallel to the polymer chains. Indeed, the alkyl tail takes the same position on the PE surface that a polymer chain would take in the bulk, so it may be assumed that the interaction is extremely favourable. The orientation of the core might then be expected to result from an interplay between the shape of the 8CB molecule and the detailed nature of the underlying surface. In fact it is the converse which is true, in that the molecular shape appears to adapt itself to suit its local environment.

The minimum energy conformation of the liquid crystal molecule corresponds to an angle of approximately 145° between the tail and the core. This appears to be consistent with the ODFs shown for the (1 1 0) surface, but not the (1 0 0) surface, on which the molecule appears to be somewhat straighter. In fact, the average shape of the molecule, defined in this case as the angle between the core and the tail, is best deduced directly

Table 3. Positions of the main peaks of the ODFs for the tails and cores of isolated 8CB, 5CB and CB molecules on a range of polymer surfaces. There is an uncertainty in all peak positions of the order of ± 5°. The polymer chain axis corresponds to 0° and 180°. In the Model column, UA = United Atom and EH = Explicit Hydrogen.

Surface	Molecule	Model	Electrostatics	Core angles/°	Tail angles/°
PE (1 1 0)	8CB	UA	No	25, 170, 205, 340	0, 180
		EH	No	150, 210, 330	0, 180
PE (1 0 0)	8CB	UA	No	10, 150, 190, 330	0, 180
		EH	No	0, 30, 150, 210, 330	0, 180
	5CB	UA	No	15, 150, 195, 325	0, 180
	CB	UA	No	15, 145, 195, 325	0, 180
PVA (1 0 0)	8CB	UA	Yes	35, 175, 205, 350	0, 185
		UA	No	0, 30, 180, 215	0, 180
Nylon 6 (0 1 0)	8CB	UA	No	30, 170, 210, 350	5, 180
PP (1 1 0)	8CB	UA	No	55, 90, 170, 235, 270, 345	60, 240

from the angular distribution shown in figure 5 for an 8CB molecule on the (1 0 0) face of PE. The distribution is broad, implying that the molecule is quite flexible, with most conformations being in the range 135° to 180°; the average angle is 142°. Figure 5 also shows the shape distribution for 8CB molecules from a monolayer simulation. The distribution is much narrower than in the single molecule simulation, with most conformations being in the range 155° to 180° and an average value of 168°. Thus, it is clear that both the presence of a substrate, and other molecules, are influencing the shape of the liquid crystal molecule. Any agreement between the core orientation implied by the minimum energy conformation, and the preferred angle in the ODF would appear to be coincidental, since figure 4 (*b*) shows clearly that the core orientations are independent of the presence of a tail.

On close examination, it is clear that the crystalline PE surfaces can be thought of as corrugated at the molecular level. In fact, the shape and depth of the corrugations vary, depending on the crystal face and the choice of model used to represent the hydrogen atoms, as demonstrated in figure 6, which shows cross sections through the Connolly surfaces [46] in each case. It can be seen that the corrugations on the (1 0 0) surface vary in depth from approximately 3 Å for the united atom model to 4.5 Å for explicit hydrogens. On the other hand, the corrugations in the (1 1 0) surface only range between 3.3 Å for united atoms and 2.8 Å for explicit hydrogens. Thus, the choice of model is likely to be more important when examining the preferred orientations on the (1 0 0) surface than on the (1 1 0) surface, as we have observed.

From inspection of the simulation trajectories, it is clear that when the angle of the core is within 15° of the polymer chain axis, the core lies entirely within one corrugation. However, when the core angle is greater than 15°, the biphenyl is actually straddling the ridge between two corrugations. This is made possible through an adjustment of the torsional angle between the two phenyl rings in the biphenyl core in order to achieve a close contact between the whole molecule and the substrate. The four principle orientations of an 8CB molecule on the (1 0 0) surface of PE are shown in figure 7.

Further insights into the preferred orientations of the CB core may be obtained by examining the variation in potential energy during the simulation. Figure 8 (*a*) shows the ODF for the CB molecule on the (1 0 0) surface of PE plotted using rectangular axes, with the non-bonded contribution to the potential energy superimposed on the same axes. It is clear that the preferred orientations correspond to the lowest energies, which are approximately -16 kcal mol^{-1} at the bottom of the potential wells. However, it is interesting to note that there are energy maxima when the molecule is both parallel and perpendicular to the chain axis. The parallel configuration is approximately 1 kcal mol^{-1} higher in energy than the lowest energy configuration, while the perpendicular configuration is approximately 2 kcal mol^{-1} higher. A similar plot is shown in figure 8 (*b*) for the core of an 8CB molecule. However, this time the non-bonded potential energy shown includes contributions from the alkyl tails. It can be seen that, whereas there is still a maximum in energy corresponding to the perpendicular orientation, the parallel orientation is now of similar energy to the two preferred off-axis orientations. The average energy of the lowest energy configurations is -18 kcal mol^{-1}, while the perpendicular configurations are, on average, 7 kcal mol^{-1} higher. Thus, the presence of the tail appears to have two effects on the liquid crystal molecule. Firstly, it makes the parallel orientation of the core more feasible energetically, and secondly, it makes the perpendicular orientation appear less likely.

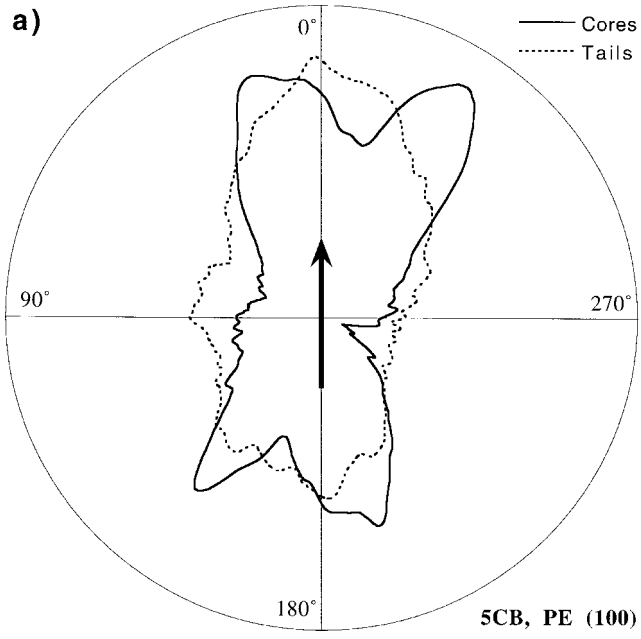

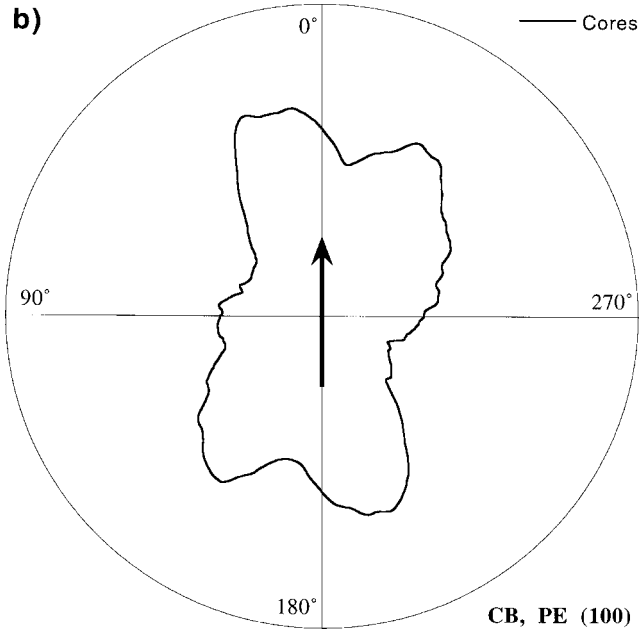

Figure 4. (*a*) ODFs for the cores and tails of a 5CB molecule on the (1 0 0) surface of PE. (*b*) A similar plot for the CB core on the same surface.

3.2. *Alkyl tail conformations*

It is well known that the conformations of macromolecules are modified by the presence of a wall or other barrier [47], and it would seem quite likely, therefore, that the alkyl tails of the liquid crystal molecules will be similarly affected by the presence of a polymer surface. Indeed, there was some concern that the presence of a substrate might bias the conformations of the liquid

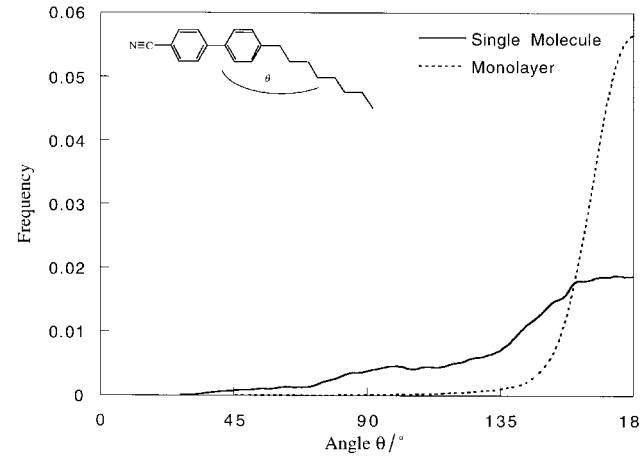

Figure 5. Distribution of angles observed between the cores and tails of 8CB molecules on the (1 0 0) surface of PE. The angle referred to is shown on the inset molecule. The solid line corresponds to a single molecule simulation, while the dashed line is taken from a monolayer simulation.

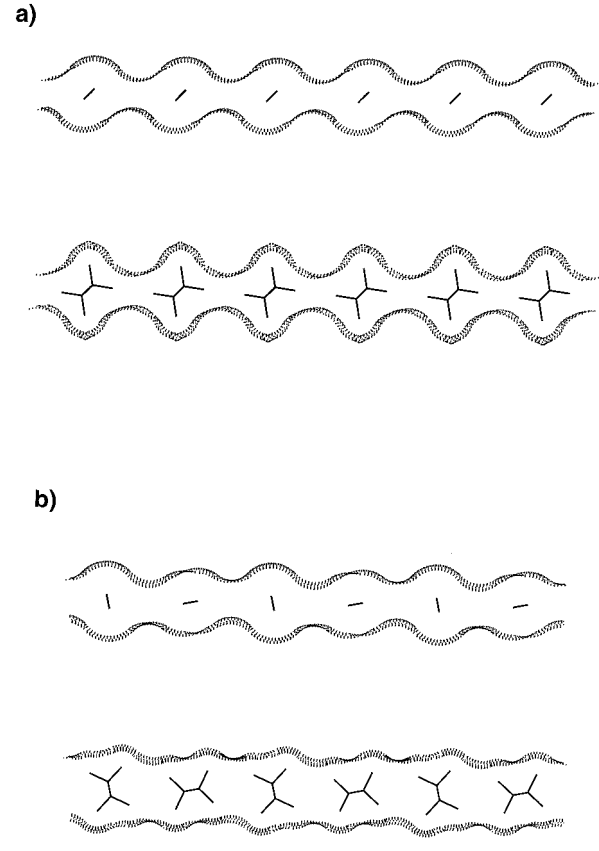

Figure 6. View looking down the chain axes for (*a*) the (1 0 0) and (*b*) the (1 1 0) crystal faces of PE, showing a molecular (Connolly) surface to indicate the size of the surface corrugations. Each surface is shown using both united atoms (top) and explicit hydrogen atoms (bottom). Molecular images created using Cerius[2].

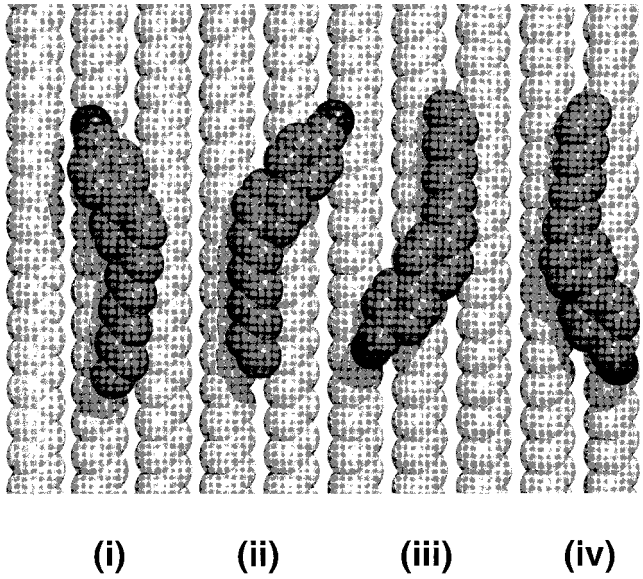

Figure 7. The four principal preferred configurations of 8CB molecules on the (1 0 0) surface of PE. Molecules (i) and (iv) are non-straddling configurations, corresponding to core angles of 10° and 190° on the ODF in figure 3(*a*). Molecules (ii) and (iii) straddle the corrugations and correspond to core angles of 150° and 330°. Molecular images created using Cerius[2] and rendered using PovChem.

crystal molecule to the extent that it might be unable fully to explore phase space. This effect was investigated by examining the torsional angle distributions for all of the carbon atoms in the alkyl tail of an 8CB molecule *in vacuo*, and comparing them with the distributions found when in contact with the (1 0 0) surface of PE, and when part of a monolayer is in contact with the same surface. The results are shown in figure 9.

It is clear in the vacuum simulation that the *trans*-conformation is favoured over the two *gauche*-states. In fact, the carbon–carbon bonds spend approximately 48% of their time in the *trans*-conformation and 26% in each of the *gauche*-conformations. However, when the 8CB molecule comes into contact with the PE surface, the alkyl tail straightens and the distribution changes to 57% for the *trans*-state and 21.5% for each *gauche*-state. Interestingly, the positions of the *gauche*-maxima also shift slightly, presumably due to the perturbing influence of the non-bonded interactions with the substrate. When the 8CB molecule forms part of a monolayer, the proportion of *trans*-conformations decreases again (*trans* = 50%, *gauche* = 25%) as the molecule deforms to attain a closer packing. This is commented on further below.

Thus, it would appear that the presence of a polymer surface does, indeed, change the distribution of *trans*- and *gauche*-states in the 8CB alkyl tails, slightly favouring the straighter chains. However, the effect is not great,

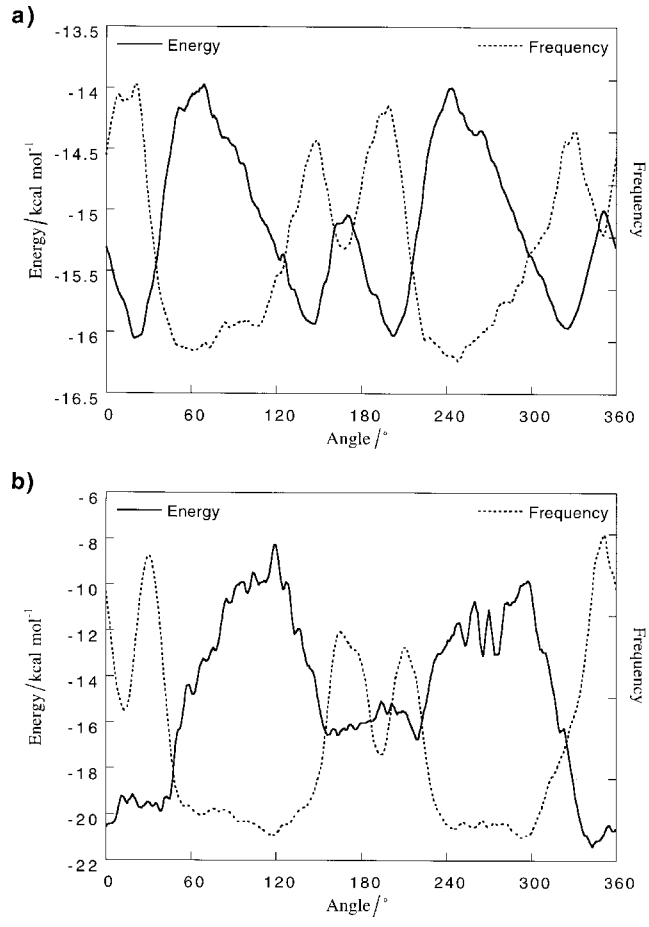

Figure 8. (*a*) The non-bonded contribution to the potential energy of a CB molecule on the (1 0 0) surface of PE as a function of orientation (solid line), with the ODF shown on the same axes for comparison (dashed line). (*b*) A similar plot for an 8CB molecule. The potential energy shown is the non-bonded contribution from the *whole* molecule, whereas the ODF shown is for the core only.

and is unlikely to prevent the liquid crystal molecule from adequately sampling phase space.

3.3. *Isolated 8CB molecules on PVA, Nylon-6 and PP*

In order to assess whether the simulations performed using PE substrates are representative of the behaviour that can be expected from polymer/liquid crystal systems in general, further simulations were performed using 8CB molecules on PVA, Nylon 6 and PP surfaces. The ODFs for 8CB molecules on the (1 0 0) surface of PVA are shown in figure 10(*a*) and table 3 with and without electrostatic interactions. The effect of electrostatic interactions appears to be very small, with the differences in peak height being mainly attributable to poor sampling statistics. In both cases, it can be seen that the main peaks for the cores are almost parallel to the polymer chain directions, with an additional small peak at *c*.30° to the polymer axis.

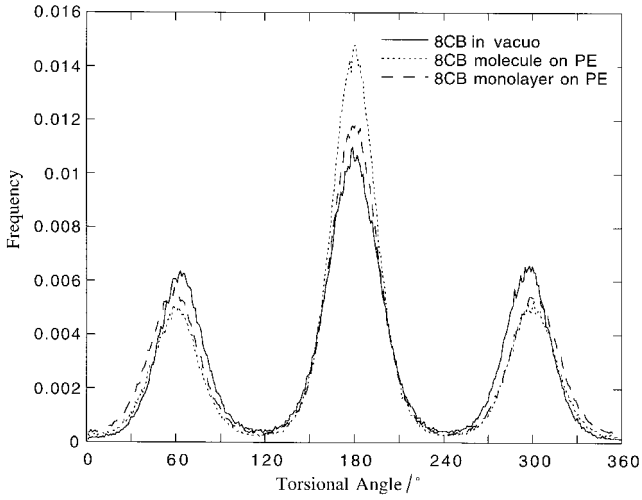

Figure 9. Torsional distributions averaged over all of the carbon–carbon bonds in the alkyl tail of an 8CB molecule under different simulation conditions: 8CB molecule in vacuo (——); isolated 8CB molecule on (1 0 0) surface of PE (.....); 8CB molecule within monolayer on (1 0 0) surface of PE (------). In this plot, the *trans*-conformation is centred around 180°, whereas the two *gauche*-conformations are centred around 60° and 300°.

The alignment of 8CB on PVA substrates contrasts with that seen on PE substrates, where only the tails showed a strong tendency to align parallel to the chain direction. The difference in alignment appears to be related to differences in the structures of the surfaces. The polymer chain separation in the PE surfaces is about 5 Å, compared with 5.5 Å for PVA, and the back-bone of the polymer chain makes a larger angle with the surface in PVA than in PE. The result is that the molecular corrugations in the PVA surface have a larger separation and steeper side walls than in PE. This allows the 8CB molecule to lie more easily within a corrugation with both the tail and the core aligned, see figure 10 (*b*). Inspection of the molecular dynamics trajectories indicates that this behaviour is facilitated by the formation of *gauche*-defects in the tail. The secondary peak in the ODF for PVA appears to be due to the core occasionally straddling the PVA chains in the same way as on the PE surfaces.

The ODFs for molecules of 8CB on the (0 1 0) surface of Nylon 6 are shown in figure 11 (*a*) and summarised in table 3. The alignment on Nylon 6 is very similar to that on the (1 0 0) surface of PE, although the main peak for the tail is rather broader than on PE. There are two factors which affect the alignment of 8CB on nylon. Firstly, the chains are closer together than in both PE and PVA with a separation of ~4.0 Å. Secondly, the plane of the chains is inclined at only ~7° to the surface, which reduces the depth of corrugations. The combination of these effects means that the behaviour

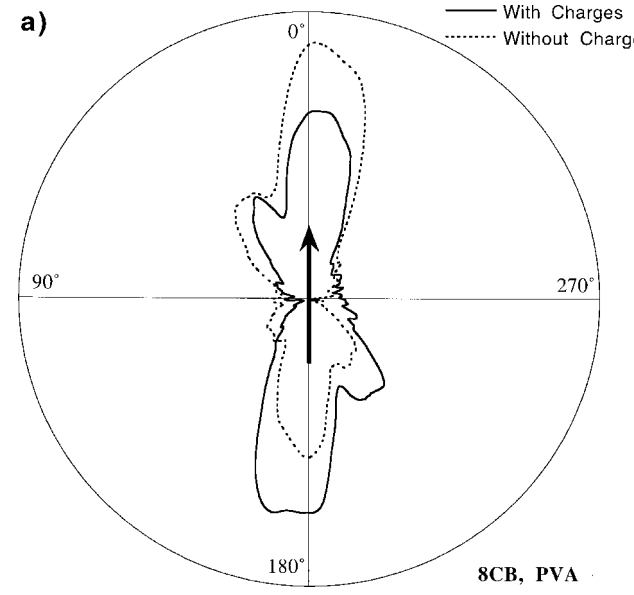

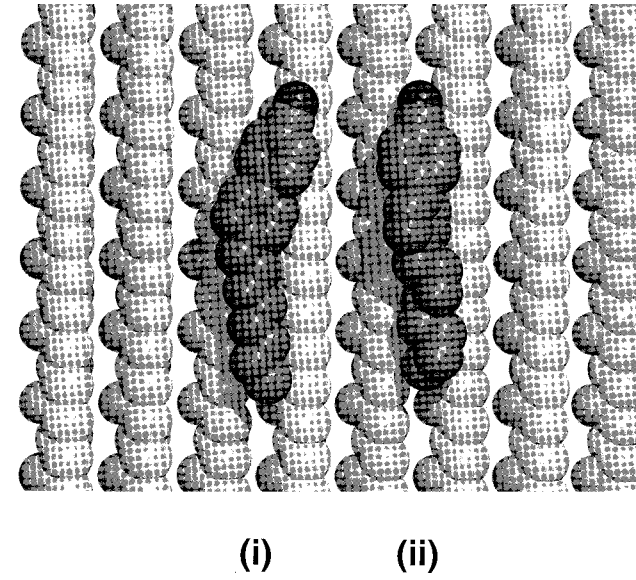

Figure 10. (*a*) ODFs for the core of an 8CB molecule on a PVA substrate with and without electrostatic interactions. (*b*) Two configurations of an 8CB molecule on the PVA substrate. In molecule (i), neither the core nor the tail are aligned parallel to the polymer chains. In molecule (ii) the introduction of *gauche*-defects in the tail enables the molecule to achieve a near parallel alignment. Molecular images created using Cerius[2] and rendered using PovChem.

is more similar to that of PE than PVA. The increased spread of the tail peak is also a result of the reduced surface corrugation.

The ODF for an isolated 8CB molecule on the (1 1 0) surface of PP is shown in figure 11 (*b*). The plots are very irregular for both the tails and the cores, showing many possible orientations, both parallel and perpendicular to the chain axes, as well as at intermediate angles.

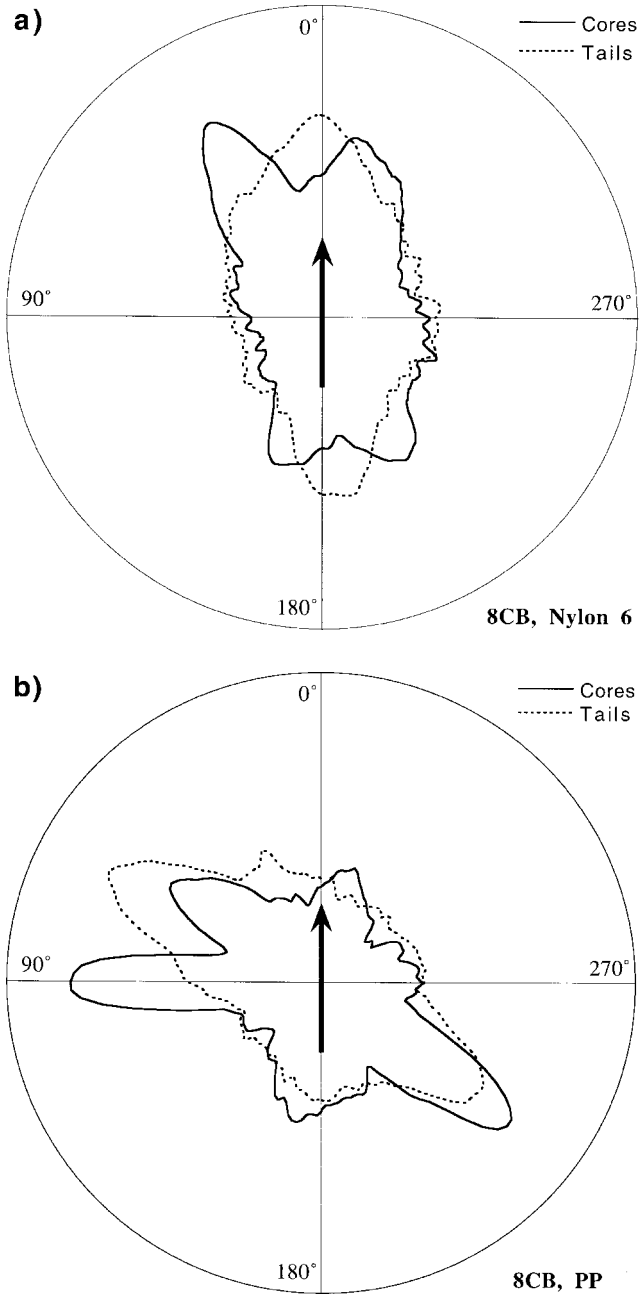

Figure 11. ODFs for an 8CB molecule on (*a*) a Nylon 6 substrate and (*b*) a PP substrate.

3.4. *Simulations of liquid crystal monolayers on PE surfaces*

The simulations of isolated liquid crystal molecules provide a relatively rapid guide to the alignment preferences of each molecule. However, since liquid crystallinity is essentially a cooperative effect, it is important to consider the effect of neighbouring molecules on the orientational behaviour. Thus, as a first step towards modelling the alignment of the bulk liquid crystal phase, simulations were performed for liquid crystal monolayers in contact with PE surfaces.

The simulations were performed using both 8CB and 5CB molecules. A typical starting configuration consisted of two rows of nine liquid crystal molecules, placed on the PE surface with their tails parallel to the polymer chains in accordance with the results from single molecule simulations. The molecules were arranged either all facing the same way on the surface [uniform configuration, figure 12(*a*)], or randomly with cores adjacent to cores *or* tails [random configuration, figure 12(*b*)). In both models, the liquid crystal cores were initially offset by about 20° from the polymer chain direction.

As can be seen from table 4 and figure 13(*a*), the ODF for the cores and the tails has changed significantly from the single molecule simulations. In particular both

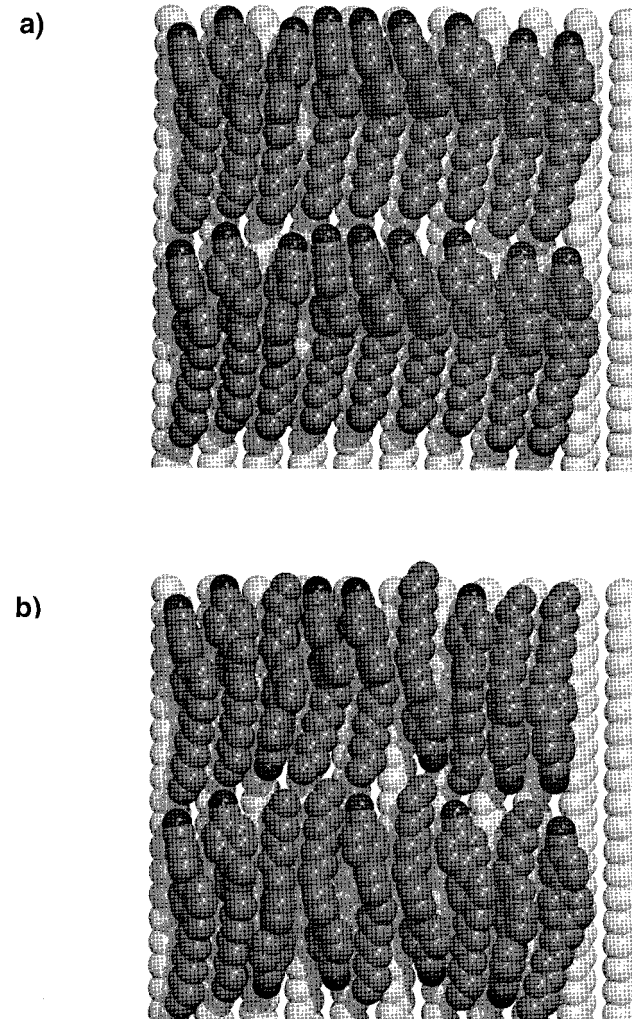

Figure 12. Typical starting configurations for the simulations of a monolayer of 18 8CB molecules on the (1 0 0) surface of PE with the molecules in (*a*) a uniform configuration and (*b*) a random configuration. Molecular images created using Cerius[2] and rendered using PovChem.

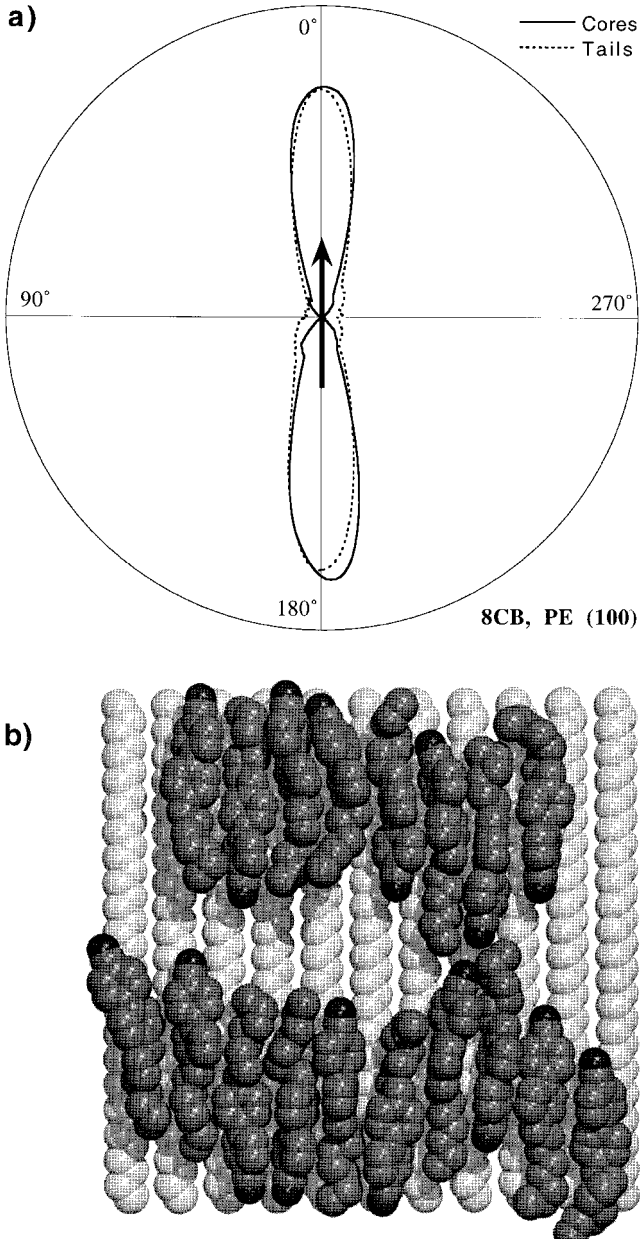

Figure 13. (*a*) ODF for the tails and cores for a monolayer of 8CB molecules on the (1 0 0) surface of PE, with the molecules in a random starting configuration. (*b*) Typical configuration taken from the simulation in (*a*). Molecular images created using Cerius[2] and rendered using PovChem.

the cores and tails now show a strong preference for aligning parallel to the chain direction, with the distributions decaying almost to zero for other orientations. The ODFs for the (1 0 0) and (1 1 0) surfaces are virtually identical, and there is essentially no difference in order between the simulations with molecules in random or uniform starting configurations. A typical configuration from a simulation with random starting configuration is shown in figure 13(*b*).

The ODFs for the monolayers of 5CB molecules closely resemble those for the 8CB monolayers (see table 4), again showing little difference between the (1 0 0) and the (1 1 0) surfaces. The main difference between the two molecules lies in the behaviour of the tails. On both surfaces, the 5CB tail distributions are around twice as wide as those for the 8CB tails, which is consistent with the single molecule results, and indicates that the 5CB tails are less well anchored than the 8CB tails.

The lateral pair correlation function for the 8CB molecules on the (1 0 0) surface is shown in figure 14. The function is very regular, with sharp peaks at an average spacing of 4.9 Å, which coincides with the spacing of the polymer chains in the surface. The regularity and sharpness of this plot indicates considerable positional ordering of the molecules. In fact, the order observed is rather greater than would be expected for either a smectic A or nematic mesophase. The orientational order parameters for most of the monolayer simulations are > 0.8, which is, again, much higher than would be expected for a nematic or a smectic A phase [18]. We attribute this to the effects of confinement by the molecular corrugations of the polymer surface.

The picture that emerges from these simulations is that, by packing the molecules side-by-side on the polymer surface, the mesogenic cores have been confined to align parallel with the polymer chains and, as a result, the whole molecule has been forced to straighten. This finding is confirmed by the plot representing the shape of the molecules which shows that most molecules have an angle between 160° and 180° between the tail and core, see figure 5. It is also supported by the observation, from the torsional distributions in figure 9, that the *trans*-conformation is slightly less common in the alkyl tails in the monolayer simulation than in the single molecule

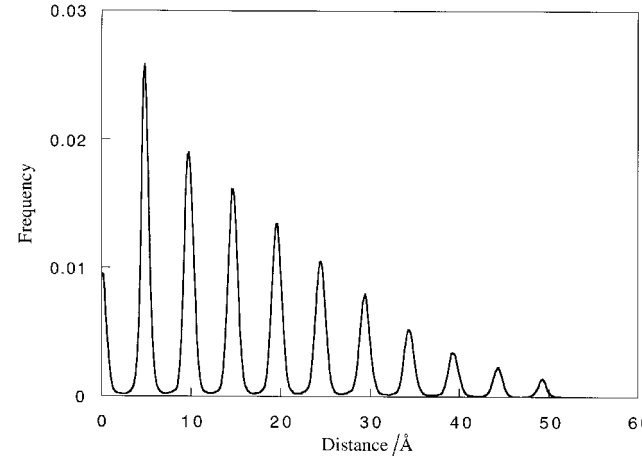

Figure 14. Lateral pair-wise correlation function for the centres of mass of 8CB molecules in a monolayer simulation on the (1 0 0) surface of PE. Uniform starting configuration.

Table 4. Positions of the ODF peaks for simulations of monolayers of 8CB and 5CB molecules on the (1 0 0) and (1 1 0) surface of PE. All angles are accurate to ± 2°. The average orientational order parameters for the molecular cores, calculated with respect to the chain direction, are also given, as well as the peak widths at half height for the tail ODFs.

Surface	Liquid crystal	Starting configuration	Core angles/°	Tail angles/°	Average tail peak width/°	Order parameter $\langle P_2 \rangle$
(1 0 0)	8CB	Uniform	2	0	18	0.92
		Random	2, 180	0, 180	20	0.90
	5CB	Uniform	355	0	39	0.92
(1 1 0)	8CB	Uniform	5	0	13	0.82
		Random	3, 182	0, 180	17	0.70
	5CB	Uniform	5	0	33	0.84

simulation; this we would expect, as the alkyl tails will also need to twist in order to accommodate the close packing. In addition, it appears that the orientations of groups of molecules are relatively insensitive to the exact details of the surfaces, in contrast to the behaviour of the single molecules. The monolayer could be thought of as a disordered epitaxial crystalline layer because it possesses considerably more regularity than would be expected for a liquid crystalline phase.

3.5. *Convergence of the monolayer ODFs*

The preceding analysis of the monolayer ODFs shows a strong tendency for the liquid crystal molecules to align parallel to the substrate chain axis. Since this direction is close to the initial orientation of the liquid crystal molecules, there may be some concern that the simulation is not showing equilibrium behaviour, but rather is stuck in a configuration close to the starting point. In order to investigate this possibility, we performed an additional simulation consisting of 18 8CB molecules on the (1 0 0) surface of PE, arranged so that the axes of the mesogenic cores were initially at 45° to the substrate chain axis. The evolution of the molecular arrangements and the ODFs were then followed, and this is summarized in figure 15.

It is clear that the ODF is initially broad, with peak widths in excess of 40°, and centred on angles at 45° to the polymer axis, see figure 15(*a*). However, the situation changes rapidly, and after 100 ps the ODF has become centred on the chain axis, with a peak width of approximately 20°, see figure 15(*b*). The shape of the ODF then remains substantially unchanged for the remainder of the simulation (1 ns), apart from the statistical fluctuations one might expect from using short sample times, see figures 15(*c–f*). The same behaviour is observed in the snapshots of configurations. It is clear that most of the reorientation which takes place occurs during the first 100 ps of the simulation. It is also clear that the liquid crystal molecules are free to rotate during the simulation but that, once they are oriented parallel to the substrate axis, they prefer not to do so. It would appear, therefore, that it is appropriate to use an equilibration time of 100 ps in the monolayer simulations, since this is approximately the time it takes for the monolayer to lose any memory of its initial orientation.

3.6. *The effect of temperature*

In the above simulations, a single temperature of 300 K was used. At this temperature, 8CB should be in the smectic A phase and 5CB should be in the nematic phase. However, as indicated above, the lateral pair correlation functions suggest a degree of order that is closer to crystalline. This finding may be compared to experimental studies of 8CB on graphite by STM which shows a similarly high degree of order [10–13]. In addition, second harmonic generation measurements have shown that 8CB molecules adsorbed on an aligning polymer substrate in a liquid crystal cell, can remain in the smectic phase up to at least 20°C above the temperature at which the bulk changes phase [48]. For this reason, a limited study of the effect of temperature on monolayers of 8CB on PE was felt appropriate.

Models were prepared consisting of four banks of six 8CB molecules in a uniform configuration on the (1 0 0) surface of PE, see figure 16. Simulations were performed at 300, 310 and 340 K, at which temperatures 8CB should be in the smectic A, nematic and isotropic phase, respectively.

The variation in the ODFs due to temperature was found to be negligible, with the shapes and positions of the peaks being virtually unchanged for both the tails and the cores. The only change found was in the longitudinal correlation function, which indicates the translational freedom of the molecules parallel to the polymer chain axis, and shows how well the banks of molecules are defined, see figure 17. The peaks in the plot correspond to the average separation of the banks of molecules, or smectic layers. As the temperature is increased, the peaks broaden very slightly and their amplitudes decrease. However, the difference is too small

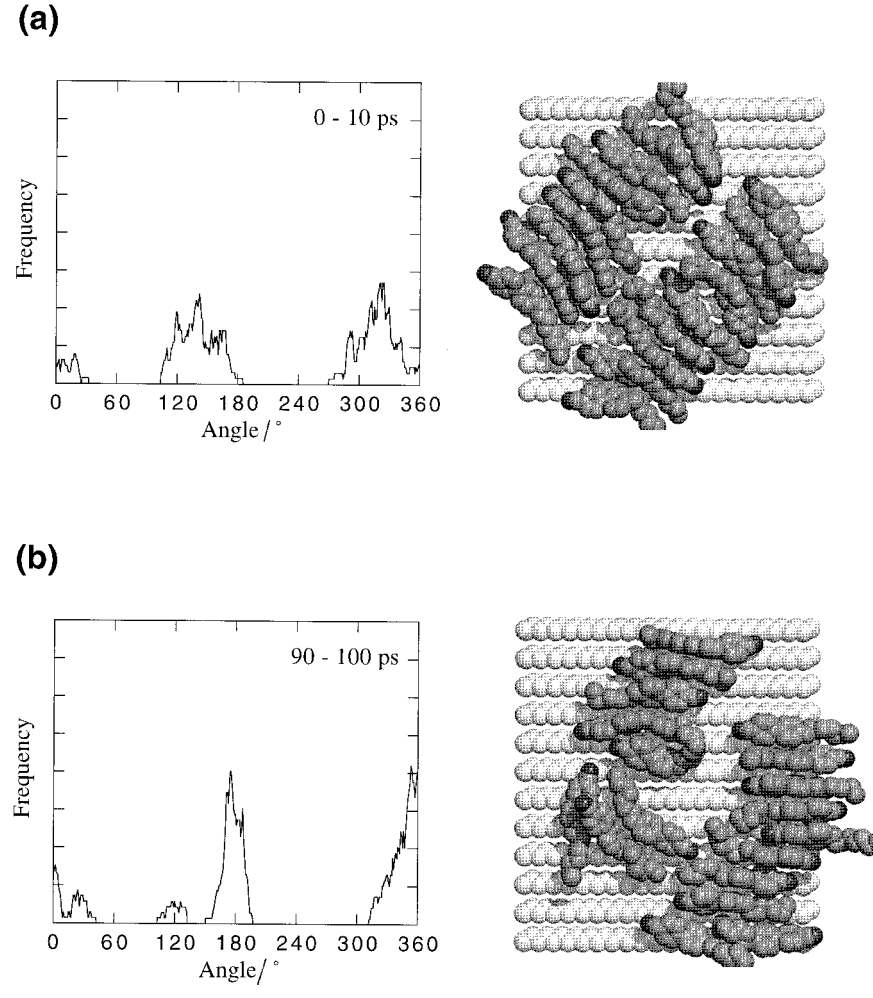

Figure 15. ODFs and snapshots of configurations taken at intervals from a simulation of 18 8CB molecules on the (1 0 0) surface of PE. The ODFs were calculated for the mesogenic cores of the 8CB molecules. The liquid crystal molecules were initially oriented with their mesogenic cores at 45° to the substrate chain axis, in the plane of the polymer surface. The ODFs were each averaged over 10 ps and are presented as rectangular plots for clarity. The total simulation time was 1 ns. (*a*) 0–10 ps; (*b*) 90–100 ps; (*c*) 190–200 ps; (*d*) 290–300 ps; (*e*) 390–400 ps; (*f*) 490–500 ps. Molecular images were created using Cerius[2] and rendered using PovChem.

to indicate any change of phase. Thus it appears that the interfacial structure is independent of the simulation temperature over a 40 degree range, although it is possible that the presence of a bulk liquid crystal phase could modify this behaviour.

3.7. *Simulations of two liquid crystal monolayers on PE*

In the monolayer simulations, it is likely that the monolayer is showing an increased adsorption onto the substrate due to the lack of bulk liquid crystal to provide a balancing force. It is also possible that this may be responsible for the high degree of order that has been observed in the system. Therefore, in order to attempt to model the effect of the bulk, simulations were performed using two monolayers, each consisting of four banks of eight 8CB molecules, i.e. 64 molecules in total. A random starting configuration was constructed using the (1 0 0) surface of PE, which is shown in figure 18. A simulation of a single layer with 32 8CB molecules was also performed with its starting configuration taken from the 64 molecule simulation, in order to provide an exact comparison between a monolayer simulation and the first layer of a two layer simulation.

ODFs for the liquid crystal monolayers are shown in figure 19. The positions of the peaks, their widths and orientational order parameters are shown in table 5. The distributions are all sharp and well defined, with a strong tendency for both the cores and the tails to align parallel with the polymer chains in the substrate.

The peaks in the ODFs for the molecules in the second layer are smaller and broader than those for the first layer, indicating a drop in orientational order on moving away from the substrate. This is reflected in a decrease in order parameter from 0.95 for the first monolayer to 0.86 for the second monolayer. The ODFs for the tails show a doubling in the peak width whilst the cores show only a 50% increase in the second layer compared with the first, indicating that the reduction in the correlation of the second layer with the surface is primarily due to the tails.

Further differences between the layers are shown by the lateral correlation functions, figure 20. The correlation

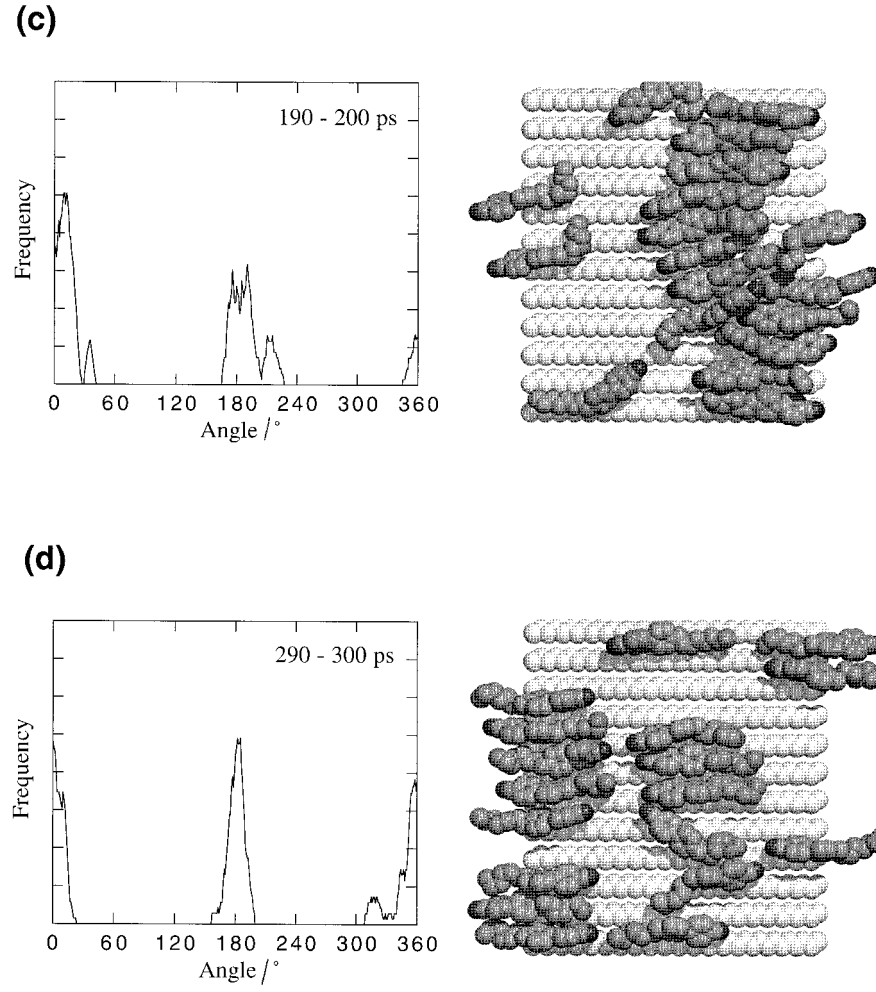

Figure 15. (*Continued*).

function for the first layer has very sharp peaks with a spacing of 4.9 Å, pointing to a high degree of correlation between the molecules and the polymer chains in the first layer. The correlation function for the second layer, on the other hand, shows a drop in the amplitude of the peaks with significant broadening. Thus, the molecules have much greater lateral mobility in the second layer than in the first.

The ODF for the single monolayer simulation is virtually identical to that for the first layer of the 64 molecule simulation, suggesting that the first layer in the 64 molecule simulation is certainly not strongly affected by the presence of the second layer of molecules. In fact, it appears that the first layer is strongly adsorbed on the substrate, and in turn induces alignment in the second, more mobile, layer.

3.8. *Liquid crystal molecules on graphite*

Both single molecules and monolayers of 8CB were simulated on the basal plane of graphite. The ODF for an isolated molecule provides a useful contrast to those observed from the polymer surfaces, see figure 21 (*a*). Any preference in alignment should show a six-fold rotational degeneracy due to the symmetry of the surface. In fact, the distributions for both the core and the tail are isotropic with no clear alignment direction.

The monolayer simulation consisted of a group of 18 molecules arranged in a uniform configuration with two banks of nine molecules each. The molecules were initially oriented parallel to the crystallographic *a* axis, and the system was simulated for 1 ns. As can be seen, the ODF for 8CB on graphite is quite different from the ODFs on PE, see figure 21 (*b*). Although the peaks are clearly centred on a single orientation, the width of the peaks is *c*.75° compared with *c*.20° peak widths for the simulations on the PE surfaces. It is also noticeable that both the tail and the core have almost identical distributions, implying that neither dominates the behaviour of the molecule.

It appears that the distribution seen here is primarily a result of the confinement of the molecules and cooperative interactions between them rather than any

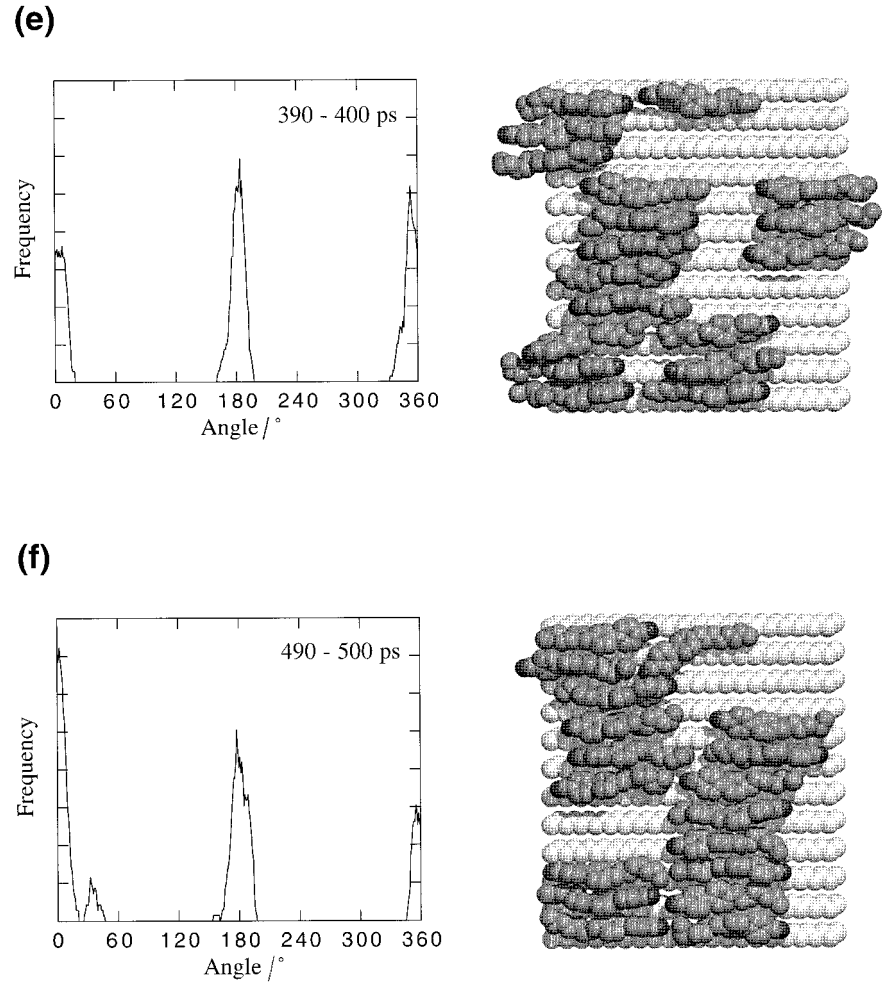

Figure 15. (*Continued*).

Table 5. Positions and peak widths from the ODFs for a two monolayer simulation of 8CB molecules on the (1 0 0) surface of PE, compared with the results for a single monolayer simulation.

System	Core angles/°	Average core peak width/°	Tail angles/°	Average tail peak width/°	Order parameter $\langle P_2 \rangle$
Layer 1	3, 177	17	0, 181	18	0.95
Layer 2	1, 180	27	0, 180	36	0.86
Monolayer	3, 177	17	0, 182	18	0.92

innate aligning ability of the graphite surface. This is demonstrated most clearly by figure 21 (*c*) which shows an ODF taken from the first 45 ps of the monolayer simulation. The ODFs for both the tail and core are relatively narrow, and centred on the initial orientation. As the simulation time is increased, the distributions broaden, as shown in figure 21 (*b*). It is likely that a further increase in simulation time would lead to a further broadening of the peaks until all orientational possibilities have been explored. The simulation shows clearly the difference between the strongly aligning surfaces of PE and a comparatively smooth one. Any orientation appears to arise from interactions between molecules keeping them all approximately parallel. This is illustrated in figure 22, which shows a typical randomly close-packed configuration. These findings also support the argument that the rather strong alignment seen for the monolayers of 8CB molecules on PE surfaces was not an artifact of the boundary conditions, i.e. the confinement of neighbouring molecules or the system size, but was undoubtedly caused by the molecular corrugations on the surfaces of the polymer crystals.

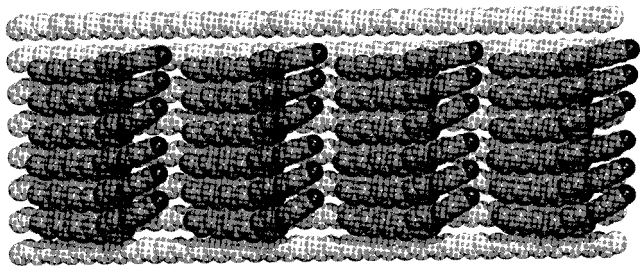

Figure 16. Starting configuration for the three simulations with 24 8CB molecules on the (1 0 0) surface of PE. Molecular images created using Cerius[2] and rendered using PovChem.

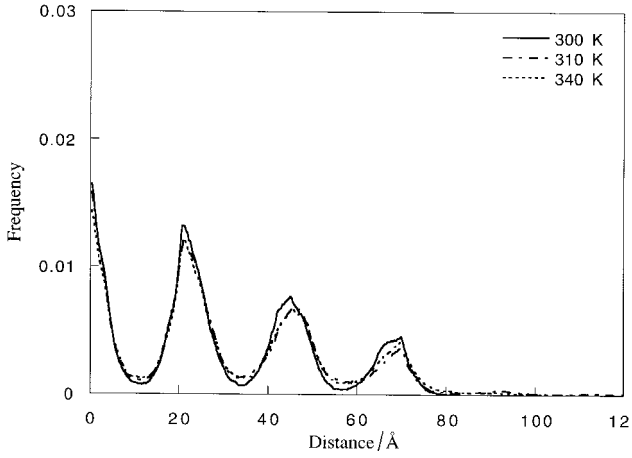

Figure 17. Comparison of the pair-wise correlation function for the molecules parallel to the chain direction for the three simulations of 24 8CB on the (1 0 0) surface of PE. The solid, dashed and dotted lines represent the simulations at 300, 310 and 340 K, respectively.

The results from these simulations disagree with STM images, which suggest that the 8CB molecules should possess a high degree of order on the basal plane of graphite. They also disagree with the results of Yoneya and Iwakabe [14], who reported a correlation between the 8CB molecules and the graphite surface in their simulations. However, recent work of Cleaver *et al.* [9] suggests that ordering of 8CB molecules is only likely to occur on a graphite substrate if the molecules are confined, for example, by the presence of an STM tip. In other words, it is possible that the order observed in the STM images is actually created by the imaging process. It is also clear from our simulations that it is important to simulate for several nanoseconds if any bias caused by the initial orientation is to be avoided. The simulations of Yoneya and Iwakabe, at 45 ps duration, may have been too short to draw any firm conclusions regarding preferred orientation.

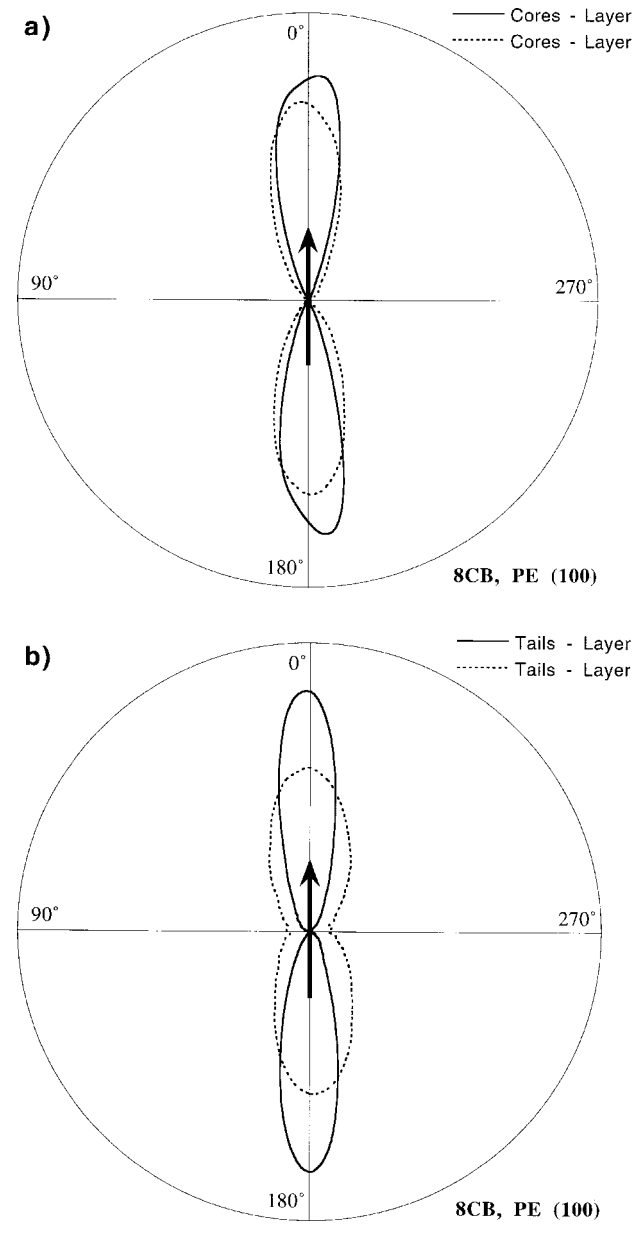

Figure 19. The ODFs for the cores and tails of 8CB molecules in a two layer simulation on the (1 0 0) surface of PE: (*a*) layer one and (*b*) layer two.

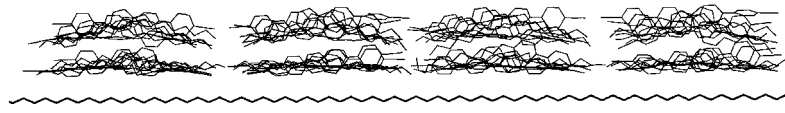

Figure 18. Side view of the starting configuration of 64 8CB molecules on the (1 0 0) surface of PE. The two layers can be seen as well as the four banks of molecules. Molecular images created using Cerius[2].

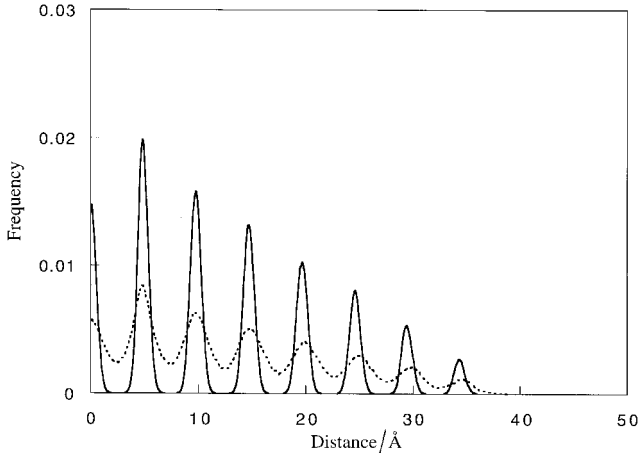

Figure 20. Lateral pair correlation function for the 8CB molecules in layers one and two calculated from the simulation in figure 19.

4. Discussion

From the above results, the simulations of isolated liquid crystal molecules appear to provide a useful guide to the aligning capabilities of polymer surfaces. PE, PVA and Nylon 6 all have, essentially, the same type of surface corrugations, with variations in aligning behaviour being attributable to differences in the width and depth of the corrugations. The exact orientation assumed by the liquid crystal cores depends on the model used for the hydrogen atoms, i.e. explicit or united atom, as this affects the shape of the corrugations; but it is clear that the use of the united atom approximation does not alter the gross behaviour of the system, i.e. whether or not alignment occurs. The united atom model therefore needs to be used with some caution but can provide useful comparative information between different systems, allowing us to demonstrate which surfaces will lead to alignment, and which will not. The ten-fold time saving involved in using united atoms makes their use highly advantageous.

The orientation preferred by the liquid crystal core also depends on the ability of the core to straddle one of the chains in the substrate, but is not directly related to the preferred angle between the core and the tail. Thus, on PE and Nylon 6, the core prefers to lie at up to 30° to the polymer chain axis in the substrate, whereas, on PVA, the nature of the corrugations are such that it is easier for the core to lie parallel to the chain axis. On PE, PVA and Nylon 6, the alkyl tail prefers to lie parallel to the chain axis, and it is clear

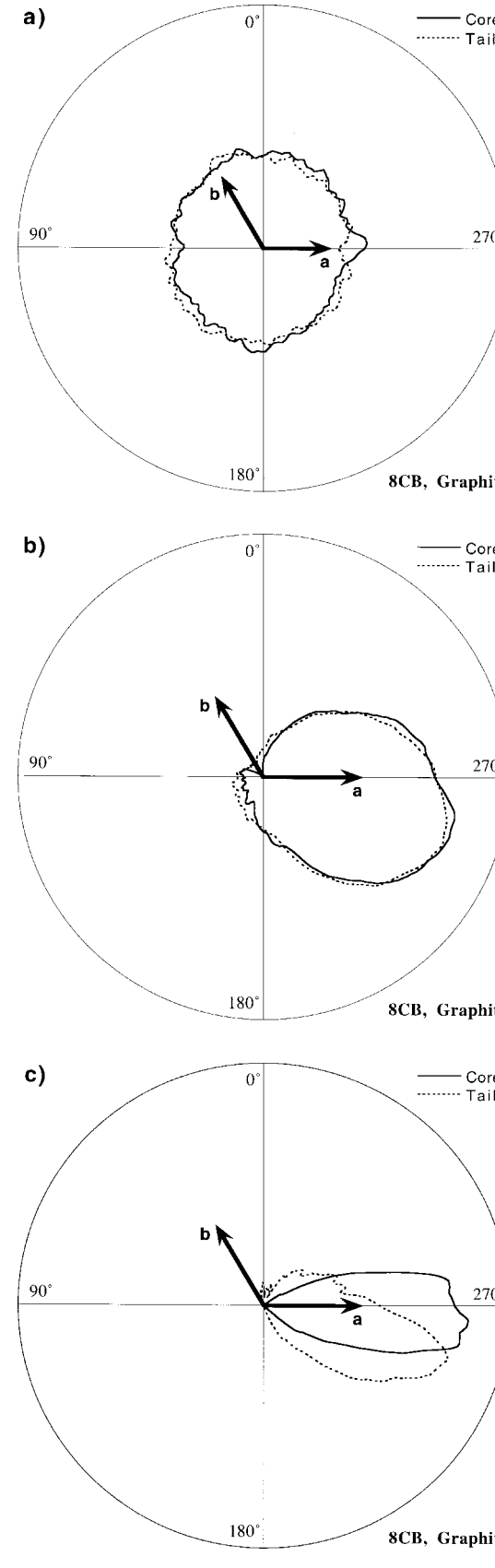

Figure 21. ODFs for 8CB molecules on the basal plane of graphite. (*a*) Single molecule and (*b*) monolayer simulations. (*c*) An ODF taken from the first 45 ps of the simulation used to generate (*b*).

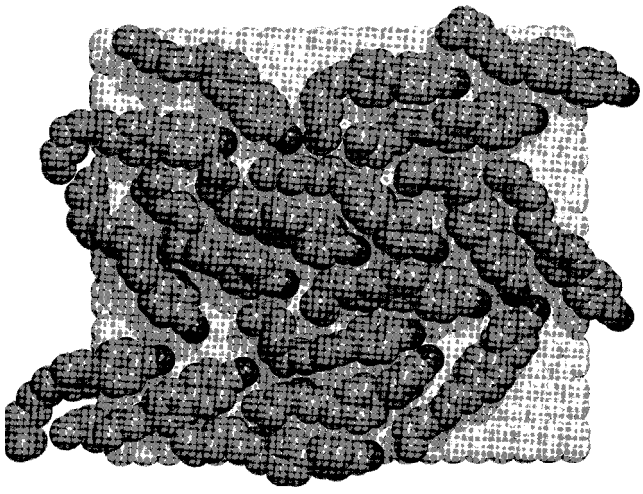

Figure 22. Typical configuration taken from a monolayer simulation of 8CB on graphite. Molecular images created using Cerius^2 and rendered using PovChem.

that the angle between the tail and the core must show considerable variability to allow for these different possibilities. In the case of the PVA surface, the core and tail are parallel, which is achieved by the introduction of gauche defects into the alkyl tail.

On PP and graphite no clear alignment preference was observed, but for different reasons in each case. On PP several orientational possibilities were found at different angles, while on graphite all orientations appeared equally likely. The difference again appears to be due to surface topography. The PP chains form helices, so that the (1 1 0) surface is actually very rough, with corrugations running in several directions. The 8CB molecules have many possible orientational choices. On the other hand, the graphite surface is much smoother than any of the polymer surfaces we examined, with the result that thermal motions are sufficient to prevent the liquid crystal molecules from aligning parallel to any of the close-packed directions.

The inclusion of electrostatic interactions appeared to make no difference to the alignment preferences, which depended almost entirely on the local topography of the model surface.

The simulations of monolayers reinforce the idea that the PE surfaces are strongly aligning. They also show that the extra confinement caused by neighbouring molecules, in conjunction with corrugations in the surface, cause the mesogenic cores to lie parallel to the chain direction and parallel to the alkyl tails. In fact, the molecules straighten by developing *gauche*, or other, defects in the conformations of the tails. This is important, since the second harmonic generation experiments which have shown that 8CB molecules align parallel to the rubbing direction [24, 48] mostly probe the orientation of the core. The subtle difference in orientation observed on the different PE surfaces for single molecules are not found in the monolayer simulations, suggesting that the behaviour of a monolayer of molecules is less sensitive to the exact nature of either the molecule or the surface.

The simulations also show that the monolayers are strongly anchored to the surface and are more highly ordered than would be expected for either a nematic or smectic A phase. Indeed, over the range of temperatures explored, little difference was observed in the ordering, suggesting that the structure at the interface may be independent of the structure of the bulk liquid crystal phase. Similar findings of excess order at liquid crystal interfaces have been reported recently by several groups [49–52]. The presence of a second monolayer did not influence the structure of the first, although the second monolayer was considerably less well ordered. It would clearly be of interest to explore how the order decreases as further monolayers are added to the system, and this will be the subject of future work.

The simulations of 8CB monolayers on graphite provide a useful illustration of the necessity of well defined molecular corrugations to induce good alignment in the liquid crystal. It is clear that the corrugations provided by the polymer chains in the crystal surfaces are of fundamental importance.

5. Conclusions

Simulations have been performed of 5CB and 8CB molecules on a variety of polymeric surfaces and graphite. Simulations of isolated molecules provide a reasonably fast indication as to whether a particular surface will induce alignment, but appear quite sensitive to the detailed structure of the polymer surface and, in particular, which model is used to represent the hydrogen atoms. Monolayer simulations, on the other hand, while considerably slower to perform, provide a more accurate estimate of the alignment orientation which appears much less sensitive to the nature of the underlying surface. Of the surfaces considered, only PE, PVA and Nylon 6 induce alignment parallel to the chain axis, or rubbing direction. PP induces many different orientations with no clear preference for either, and we failed to find any alignment preferences on the graphite surface. The ordering of the liquid crystal monolayer was considerably greater than would be expected for a nematic or smectic A phase, and indicates that the interfacial region between the aligning material and the bulk liquid crystal phase resembles an epitaxial crystalline layer rather than a liquid crystal.

We would like to thank the EPSRC, CRL and Molecular Simulations Inc. (MSI) for supporting this project through a CASE studentship. In particular, we

would like to thank MSI for unlimited access to their Cerius² molecular modelling package for the duration of the project and the loan of a computer workstation, and Dr Andreas Bick (MSI), Mr Paul Surguy (CRL) and Dr Doug Cleaver (Sheffield Hallam University) for many helpful discussions.

References

[1] Berreman, D. W., 1972, *Phys. Rev. Lett.*, **28,** 1683.
[2] Berreman, D. W., 1973, *Mol. Cryst. liq. Cryst.*, **23,** 215.
[3] Geary, J. M., Goodby, J. W., Kmetz, A. R., and Patel, S. J., 1987, *J. appl. Phys.*, **62,** 4100.
[4] Castellano, J. A., 1983, *Mol. Cryst. liq. Cryst.*, **94,** 33.
[5] Factor, B. J., Russell, T. P., and Toney, M. F., 1993, *Macromolecules*, **26,** 2847.
[6] Saraf, R. F., Dimitrakopoulos, C., Toney, M. F., and Kowalczyk, S. P., 1996, *Langmuir*, **12,** 2802.
[7] Toney, M. F., Russell, T. P., Logan, J. A., Kikuchi, H., Sands, J. M., and Kumar, S. K., 1995, *Nature*, **374,** 709.
[8] Cleaver, D. J., and Tildesley, D. J., 1994, *Mol. Phys.*, **81,** 781.
[9] Cleaver, D. J., Callaway, M. J., Forester, T., Smith, W., and Tildesley, D. J., 1995, *Mol. Phys.*, **86,** 613.
[10] Foster, J. S., and Frömmer, J. E., 1988, *Nature*, **333,** 542.
[11] Smith, D. P. E., Horber, J. K. H., Binning, G., and Nejoh, H., 1990, *Nature*, **344,** 641.
[12] Iwakabe, Y., Hara, M., Kondo, K., Tochigi, K., Mukoh, A., Yamada, A., Garito, A. F., and Sasabe, H., 1991, *Jpn. J. appl. Phys., Part 1*, **30,** 2542.
[13] McMaster, T. J., Carr, H. J., Miles, M. J., Cairns, P., and Morris, V. J., 1991, *Liq. Cryst.*, **9,** 11.
[14] Yoneya, M., and Iwakabe, Y., 1995, *Liq. Cryst.*, **18,** 45.
[15] Yoneya, M., and Iwakabe, Y., 1996, *Liq. Cryst.*, **21,** 347.
[16] Yoneya, M., and Iwakabe, Y., 1996, *Liq. Cryst.*, **21,** 817.
[17] Binger, D. R., and Hanna, S., 1999, *Liq. Cryst.* (to be published).
[18] Chandrasekhar, S., 1992, *Liquid Crystals*, 2nd Edition (Cambridge: CUP).
[19] Gray, G. W., Harrison, K. J., Nash, J. A., Constant, J., Hulme, D. S., Kirton, J., and Raynes, E. P., 1974, in *Liquid Crystals and Ordered Fluids*, edited by J. F. Johnson and R. S. Porter (London: Plenum), p. 617.
[20] Leadbetter, A. J., Durrant, J. L. A., and Rugman, M., 1977, *Mol. Cryst. liq. Cryst.*, **34,** 231.
[21] Gray, G. W., Harrison, K. J., and Nash, J. A., 1975, *Pramana Suppl.*, **1,** 381.
[22] Myrvold, B. O., 1991, *Liq. Cryst.*, **10,** 771.
[23] Van Aerle, N. A. J. M., Barmentlo, M., and Hollering, R. W. J., 1993, *J. appl. Phys.*, **74,** 3111.
[24] Barmentlo, M., van Aerle, N. A. J. M., Hollering, R. W. J., and Damen, J. P. M., 1992, *J. appl. Phys.*, **71,** 4799.
[25] Ishihara, S., Wakemoto, H., Nakazima, K., and Matsuo, Y., 1989, *Liq. Cryst.*, **4,** 669.
[26] Billmeyer Jr., F. W., 1984, *Textbook of Polymer Science*, 3rd Edn (New York: Wiley).
[27] Myrvold, B. O., 1993, *Abs. Papers Am. chem. Soc.*, **205,** 372-POLY.
[28] Young, R. J., and Lovell, P. A., 1991, *Introduction to Polymers*, 2nd Edn (London: Chapman & Hall).
[29] Parikh, D., and Phillips, P. J., 1982, *J. chem. Phys.*, **83,** 1948.
[30] Bunn, C. W., 1948, *Nature*, **161,** 929.
[31] Snétivy, D., Guillet, J. E., and Vancso, G. J., 1993, *Polymer*, **34,** 429.
[32] Snétivy, D., and Vancso, G. J., 1994, *Polymer*, **35,** 461.
[33] Bunn, C. W., 1939, *Trans. Faraday Soc.*, **35,** 482.
[34] Holmes, D. R., Bunn, C. W., and Smith, D. J., 1955, *J. polym. Sci.*, **7,** 159.
[35] Natta, G., and Corradini, P., 1960, *Nuovo Cimento, Suppl.*, **15,** 40.
[36] Cerius² v.3.5, Molecular Modelling Software, available from Molecular Simulations Ltd., 240/250 The Quorum, Barnwell Road, Cambridge CB5 8RE, UK (http://www.msi.com/).
[37] Mayo, S. L., Olafson, B. D., and Goddard, W. A., 1990, *J. phys. Chem.*, **94,** 8897.
[38] Rappé, A. K., and Casewit, C. J., 1997, *Molecular Mechanics across Chemistry* (Sausalito, California: University Science Books), pp. 34–44.
[39] Emsley, J. W., Horne, T. J., Celebre, G., Deluca, G., and Longeri, M., 1992, *J. chem. Soc. Faraday Trans.*, **88,** 1679.
[40] Komolkin, A. V., Laaksonen, A., and Maliniak, A., 1994, *J. Chem. Phys.*, **101,** 4103.
[41] Stewart, J. J. P., 1990, *J. Comput. aided Mol. Desn*, **4,** 1.
[42] Gasteiger, J., and Marsili, M., 1979, *Tetrahedron*, **36,** 3219.
[43] PovChem v.1.00, Chemical Ray Tracing Software, available from Paul Theissen (http://cherubino.med.jhmi.edu/~paul/PovChem.html).
[44] Windle, A. H., 1982, in *Developments in Oriented Polymers—1*, edited by I. M. Ward (London: Applied Science), pp. 1–46.
[45] Binger, D. R., and Hanna, S., 1997, *Mol. Cryst. liq. Cryst.*, **302,** 63.
[46] Connolly, M. L., 1983, *J. appl. Crystallogr.*, **16,** 548.
[47] DeGennes, P. G., 1979, *Scaling Concepts in Polymer Physics* (New York: Cornell University Press), pp. 88–97 and references therein.
[48] Chen, W., Feller, M. B., and Shen, Y. R., 1989, *Phys. Rev. Lett.*, **63,** 2665.
[49] Stelzer, J., Galatola, P., Barbero, G., and Longa, L., 1997, *Phys. Rev. E*, **55,** 477.
[50] Palermo, V., Biscarini, F., and Zannoni, C., 1998, *Phys. Rev. E*, **57,** R2519.
[51] Wall, G. D., and Cleaver, D. J., 1997, *Phys. Rev. E*, **56,** 4306.
[52] Del Rio, E. M., and de Miguel, E., 1997, *Phys. Rev. E*, **55,** 2916.